

Study of p_T spectra of light particles using modified Hagedorn function and cosmic rays Monte Carlo event generators in proton-proton collisions at $\sqrt{s} = 900$ GeV

Muhammad Ajaz¹, Muhammad Waqas², Guang Xiong Peng², Zafar Yasin³, Hannan Younis⁴ and Abd Al Karim Haj Ismail^{5,6}

¹ Department of Physics, Abdul Wali Khan University Mardan, 23200 Mardan, Pakistan

² School of Nuclear Science and Technology, University of Chinese Academy of Sciences, Beijing 100049, China

³ Pakistan Institute of Nuclear Science and Technology (PINSTECH) Islamabad, 44000 Islamabad, Pakistan

⁴ Department of Physics, COMSATS University Islamabad, 44000 Islamabad, Pakistan

⁵ College of Humanities and Sciences, Ajman University, 346 Ajman UAE

⁶ Nonlinear Dynamics Research Center (NDRC), Ajman University, 346 Ajman UAE

Received: date / Revised version: date

Abstract Transverse momentum spectra (p_T) of charged particles including π^\pm , K^\pm and (anti-)protons measured by ALICE experiment in the p_T range of 0.1 – 2.5 GeV/c and $|\eta| < 0.5$ are studied in pp collisions at $\sqrt{s} = 900$ GeV using modified Hagedorn function with embedded transverse flow velocity and are compared to the predictions of EPOS-LHC, Pythia, QGSJET and Sibyll models. We find that the average transverse flow velocity (β_T) decreases with increasing the mass of the particle while the kinetic freeze-out temperature (T_0) extracted from the function increases with the particle's mass. The former varies from (0.36 ± 0.01) c to (0.25 ± 0.01) c for π^\pm to protons while the latter from (76 ± 6) MeV to (95 ± 5) MeV respectively. The fit of the models predictions also yield the same values for T_0 and β_T as the experimental data. The only difference is in the values of n , and N_0 which yields different values for different models. The EPOS-LHC, Pythia, and QGSJET models reproduce the data in most of the p_T range for π^\pm , EPOS-LHC and Sibyll for K^\pm up to 1.5 GeV/c and EPOS-LHC for protons up to 1.6 GeV/c. The model simulations also reproduced the behavior of increasing average transverse momentum with mass reported by the ALICE experiment.

1 Introduction

The study of hadron production is being used in cosmic ray physics as well as in nuclear and particle physics by absolute yield, angular distributions, transverse momentum (p_T), rapidity (y) and pseudo-rapidity (η) distributions. These studies can be used to tune the event generators including but not limited to partons interaction, partons correlation, partons hadronization, collective flow, spin, and final state effects etc [1]. Furthermore, centrality dependence of the yield and hadrons spectra can be used to improve the related parameters in the modeling of the event generators.

The study of pp collisions is further relevant to the investigation of heavy-ion collisions as it is being used as a reference to find the properties of medium effect. In case of heavy-ion collisions, various final-state effects are modifying the yield as well as the spectral shape of different hadron [2,3].

A Tsallis distribution function has been used by many researchers because of its very good reproduction of the p_T spectra of experimental data at low as well as high p_T . The Tsallis distribution function is further extended by including different transverse flow models to describe the p_T spectra of hadrons produced in pp and heavy-ion collisions at high-energies. In literature, the blast-wave model coupling with Boltzmann-Gibbs statistics (BGBW model) [4,5], the blast-wave model with Tsallis statistics (TBW model) [6], the Tsallis distribution incorporating the transverse flow effect also known as Improved Tsallis distribution as well as incorporating other model functions [6,7], and Hagedorn function with transverse flow [8,9,10,11] have been used to extract the kinetic freeze-out temperature and transverse flow velocity. In continuation of [12,13,14,15,16,17,18], here we used the measurements of the charged pions and kaons, and (anti-)protons in pp collision by the ALICE collaboration at 900 GeV [19]. Simulation results of four different hadron production models are used for comparison with the data with the same cuts used by the data. Furthermore, we have used the Hagedorn function with the embedded transverse flow velocity to extract the kinetic freeze-out

temperature and transverse flow velocity.

2 The method and models

Transverse momentum spectra (p_T) of π^\pm , K^\pm , and (anti-) protons in pp collisions at $\sqrt{s} = 900$ GeV measured by the ALICE experiment [19] in the transverse momentum range of $p_T = 0.1 - 2.5$ GeV/ c and pseudorapidity region of $|\eta| < 0.5$ are investigated by using modified Hagedorn function with embedded transverse flow velocity. The measured spectra are also compared to the predictions of Cosmic Ray Monte Carlo (crmc) models including EPOS–LHC [20], Pythia [21], QGSJET [22,23], and Sibyll2.3d [24]. Simulations of one million pp collision at 900 GeV under the same condition as the data were performed by using the above event generators.

Several hadron production models are being used to simulate air showers including the ones used in this study. The advantage of these models is that they are tuned to LHC data and can be used up to 7 TeV energies for reproducing results of the experimental data. All these event generators are mainly based on simple Parton models incorporating Gribov-Regge theory. Multiple scattering approach is used in these models that are resulting exchange of multiple Parton ladders between target and projectile. Beside this, every model has a different philosophy. The EPOS model is used both for hadron-hadron, nucleus-nucleus interaction and simulation of cosmic rays air showers. It is a minimum bias hadronic interaction model aiming to describe soft particle production below 5 GeV/ c with greater details at any energy and mass of the colliding system. Several effects pertaining to heavy-ion collisions are incorporated in it such as screening [26], Cronin effect, collective effects [27], and Parton saturation. The same covariant approach is used as the previous version of the model with an improved flow parameterization. New features included in the model are described in greater detail in Ref. [20]. The Pythia Monte Carlo event generator is developed to generate interactions of high-energy particles to produce their properties in strong interaction. The code is mainly based on a different QCD-based models along with the use of some analytical results. The model incorporates processes such as hard sub processes, final- and initial-state Parton showers, underlying events, beam remnants, decays and fragmentation. A detail description of the model can be found in Ref. [21]. QGSJET model, based on Quark Gluon String (QGS) [28] model using Gribov-Regge theory, is a model commonly used for cosmic ray simulations by different group of researchers and collaborations [22] for many years.

At high energies, the transverse momentum at the high p_T tail of the hadrons spectra in hadron-hadron and nucleus-nucleus collisions is very well reproduced by QCD inspired Hagedorn function [8]:

$$\frac{d^2 N}{2\pi N_{ev} p_T dp_T dy} = C \left(1 + \frac{m_T}{p_0} \right)^{-n}, \tag{1}$$

In this expression, $m_t = \sqrt{p_T^2 + m_0^2}$, is the transverse mass with m_0 as the rest mass of a hadron, C is the constant of the fit, and n and p_0 are the two free parameters of the function to be determined. The term p_0 in Eq. 1 is equal to nT_0 , where T_0 is used to incorporate the temperature (kinetic freeze-out temperature) in the function. The equation becomes

$$\frac{d^2 N}{2\pi N_{ev} p_T dp_T dy} = C \left(1 + \frac{m_T}{nT_0} \right)^{-n}, \tag{2}$$

To incorporate the value of the collective transverse flow in Eq. 2, m_T is replaced with

$$m_T = \langle \gamma_T \rangle \left(m_T - p_T \langle \beta_T \rangle \right) \tag{3}$$

The last modification has been used by [9,10,25], the final equation becomes

$$\frac{d^2 N}{2\pi N_{ev} p_T dp_T dy} = C \left(1 + \langle \gamma_T \rangle \frac{m_T - p_T \langle \beta_T \rangle}{nT_0} \right)^{-n}, \tag{4}$$

Where C is the normalization constant which results in the integral of Eq. 4 to be normalized to 1, T_0 is the kinetic freeze-out temperature, $\langle \gamma_t \rangle = 1/\sqrt{1 - \langle \beta_t^2 \rangle}$, and $\langle \beta_t \rangle$ is the average transverse flow velocity. The last equation is known as Hagedorn function with the embedded transverse flow velocity. It is worth mentioning that the function has been used in Refs. [9,10,25]. With only a few parameters, the model has successfully described the physical parameters

Table 1. The values of free parameters (n , T_0 and $\langle \beta_T \rangle$) and normalization constant (N_0) obtained by the fit function (Eq. 5) from the p_T distribution of charged particles shown in figure 1.

Collisions	Data	Particle	T_0	β_T	n	N_0	
Fig. 1(a)	ALICE	π^+	0.076 ± 0.006	0.360 ± 0.010	7.4 ± 0.5	196 ± 12	
	ALICE	π^-	0.076 ± 0.005	0.360 ± 0.009	7.4 ± 0.5	196 ± 11.5	
pp	Epos-LHC	π^+	0.076 ± 0.005	0.360 ± 0.010	7.6 ± 0.4	220 ± 21	
	Epos-LHC	π^-	0.076 ± 0.006	0.340 ± 0.010	7.6 ± 0.8	210 ± 25	
0.9 TeV	QGSJET11	π^+	0.076 ± 0.005	0.360 ± 0.008	7.6 ± 0.6	226 ± 25	
	QGSJET11	π^-	0.076 ± 0.005	0.360 ± 0.009	7.6 ± 0.5	226 ± 19	
	Pythia	π^+	0.076 ± 0.004	0.360 ± 0.009	7.6 ± 0.6	220 ± 20	
	Pythia	π^-	0.076 ± 0.005	0.360 ± 0.008	7.6 ± 0.7	215 ± 23	
	Sibyll	π^+	0.076 ± 0.006	0.360 ± 0.008	8.6 ± 0.6	270 ± 31	
	Sibyll	π^-	0.076 ± 0.005	0.360 ± 0.008	8.6 ± 0.5	270 ± 19	
	Fig. 1 (b)	ALICE	K^+	0.086 ± 0.004	0.300 ± 0.011	6.5 ± 0.6	23 ± 2
		ALICE	K^-	0.086 ± 0.005	0.300 ± 0.011	7.5 ± 0.5	24 ± 3
pp		Epos-LHC	K^+	0.086 ± 0.006	0.300 ± 0.011	7.3 ± 0.6	22.5 ± 2
		Epos-LHC	K^-	0.086 ± 0.006	0.300 ± 0.010	7.3 ± 0.4	22.3 ± 2
0.9 TeV		QGSJET11	K^+	0.086 ± 0.005	0.300 ± 0.009	7.6 ± 0.3	20 ± 2
		QGSJET11	K^-	0.086 ± 0.005	0.300 ± 0.009	6.6 ± 0.3	20 ± 1
		Pythia	K^+	0.086 ± 0.005	0.300 ± 0.010	7.5 ± 0.4	20 ± 3
		Pythia	K^-	0.086 ± 0.005	0.300 ± 0.010	7.5 ± 0.4	22 ± 3
	Sibyll	K^+	0.086 ± 0.004	0.300 ± 0.010	7.7 ± 0.7	24 ± 3	
	Sibyll	K^-	0.086 ± 0.004	0.300 ± 0.010	8.6 ± 0.7	20 ± 4	
Fig. 1(c)	ALICE	p	0.095 ± 0.005	0.250 ± 0.010	8 ± 0.5	10 ± 0.6	
	ALICE	\bar{p}	0.095 ± 0.005	0.250 ± 0.010	8 ± 0.5	10 ± 0.6	
pp	Epos-LHC	p	0.095 ± 0.006	0.250 ± 0.010	8.8 ± 0.6	10 ± 0.4	
	Epos-LHC	\bar{p}	0.095 ± 0.005	0.250 ± 0.010	8 ± 0.5	10 ± 0.3	
0.9 TeV	QGSJET11	p	0.095 ± 0.005	0.250 ± 0.009	7.6 ± 0.3	10 ± 2	
	QGSJET11	\bar{p}	0.095 ± 0.005	0.250 ± 0.009	7.6 ± 0.3	9.8 ± 1	
	Pythia	p	0.095 ± 0.004	0.250 ± 0.011	10.3 ± 0.7	11.6 ± 1.4	
	Pythia	\bar{p}	0.095 ± 0.004	0.250 ± 0.010	8 ± 0.6	10 ± 1.2	
	Sibyll	p	0.095 ± 0.005	0.250 ± 0.010	7.5 ± 0.4	10 ± 1	
	Sibyll	\bar{p}	0.095 ± 0.004	0.250 ± 0.010	7.5 ± 0.4	9.7 ± 1.1	

of the spectra as described in [9,10,25]. The current form of the modified Hagedorn function is further modified for the current analysis as follows:

$$\frac{d^2 N}{N_{ev} dp_T dy} = 2\pi p_T C \left(1 + \langle \gamma_T \rangle \frac{m_T - p_T \langle \beta_T \rangle}{n T_0} \right)^{-n}, \quad (5)$$

We used the above Hagedorn formula (Eq. 5) to fit the p_T spectra of charged pions, kaons, and (anti-)protons and extracted the parameters for the data as well as all the models for comparison.

2.1 Results and Discussion

The transverse momentum spectra (p_T) of identified charged particles measured by the ALICE experiment in the p_T range of (0.1–2.5) GeV/ c and pseudorapidity $|\eta| < 0.5$ in pp collisions at $\sqrt{s} = 900$ GeV are analysed by using a modified Hagedorn function with the embedded transverse flow velocity (Eq. 5). The results of the fit function are given in Table 1. The result of the fit curves on the p_T distributions of the particles are shown in Figures 1. The solid and hollow symbols in each panel represent the data for particles and their anti-particles respectively. Figure 1(a). shows the fit curves for the experimental data and models for π^\pm mesons, while figure 1(b) and 1(c) show the same for K^\pm and (anti-)protons respectively. The curve shows that the function fit the experimental data approximately well. In case of the pions, there is some discrepancy between the data/fit and fit function result for $p_T < 0.5$ GeV/ c , which is indicated by the Data/Fit curve shown in the lower panel of the plot. The reason behind this discrepancy is that most of the low energy pions are produced by the decay of resonance particles – an effect which is not incorporated into the function. The Data/Fit above $p_T = 0.5$ GeV/ c is around unity in Fig. 1(a) as well as in Fig 1(b) and 1(c) which shows good agreement of the fit function to the experimental data.

Table 1. shows the values of the free parameters obtained by the fit function in Eq. 5. The average transverse flow velocity ($\langle \beta_T \rangle$) decreases with increasing the mass of the particle (which is a natural hydro-dynamical behavior). It is equal to $(0.36 \pm 0.01)c$ for π^\pm , $(0.03 \pm 0.01)c$ for K^\pm mesons while $(0.25 \pm 0.01)c$ for p (\bar{p}). Similarly the value T_0 increases with increasing the mass of the particles with (76 ± 6) MeV, (86 ± 5) and (95 ± 5) MeV respectively for π^\pm , K^\pm and p (\bar{p}) which shows the mass dependent kinetic freeze-out scenario, in agreement with ref. [29,30,31,32]. The fit of the function on the models predictions also yield the same values for T_0 and β_T as the experimental data. The

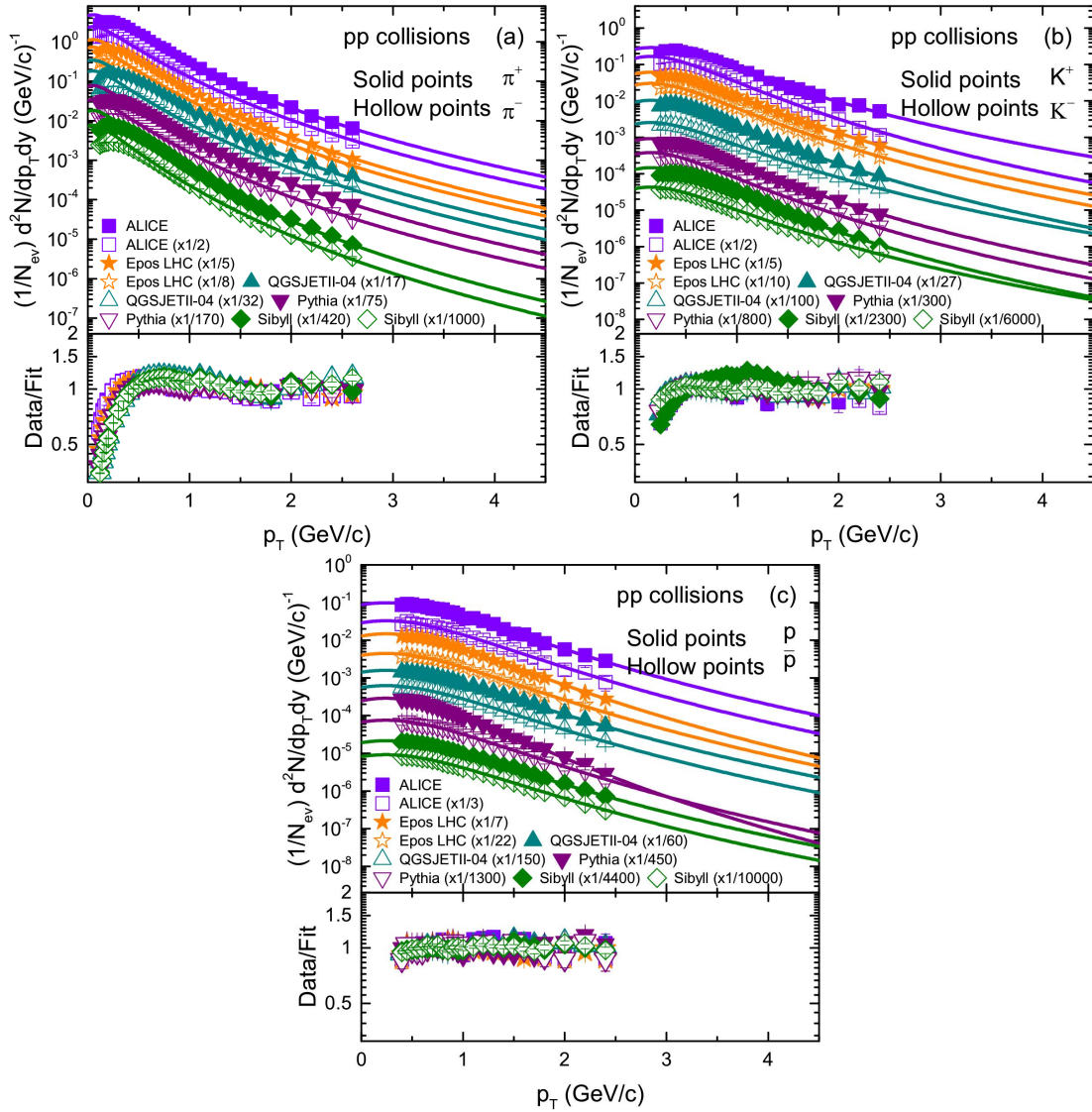


Figure 1: Result of the fit function on the transverse momentum spectra of pions (a) kaons (b) and protons (c) produced in pp collision at 900 GeV by Data, EPOS–LHC, Pythia, QGSJET and Sibyll models. Filled markers are used to represent positive particles while open markers are used to show negative particles. Lines in different colors are used to show the fit curve obtained using Eq 5.

difference between the models and data is only reflected in the difference of n and N_0 which also have comparable values. The parameter N_0 is observed to be dependent on the mass of the particle. The parameter n is connected to the scattering centers involved in the interaction process and yield a higher value for multiple scattering center, while N_0 is the fit constant which is used for the comparison of the fit function. It should be noted that the normalization constants C in Eq. 5 and N_0 in table 1 are not the same. C is the normalization constant which is used to let the integral of Eq. 4 be 1, while the normalization constant N_0 is used to compare the fit function and the experimental spectra. The constant C can be absorbed in N_0 , but we have used both C and N_0 to give a clear description. The parameter N_0 has its physical significance. It reflects the multiplicity. In the present work, we found that N_0 is larger for pions, followed by kaons, while protons have the lowest value for N_0 which means that pions have larger multiplicity and protons have the lowest multiplicity. This result is in agreement with [33].

Transverse momentum spectra of the positively charged (left column) and negatively charged (right column) pions (first row) kaons (second row) and protons (third row) produced in pp collision at 900 GeV by EPOS–LHC, Pythia, QGSJET and Sibyll models are compared with the measurement of ALICE experiment. The solid black markers represents experimental data while line of different colors are used to show the models result highlighted in the legend

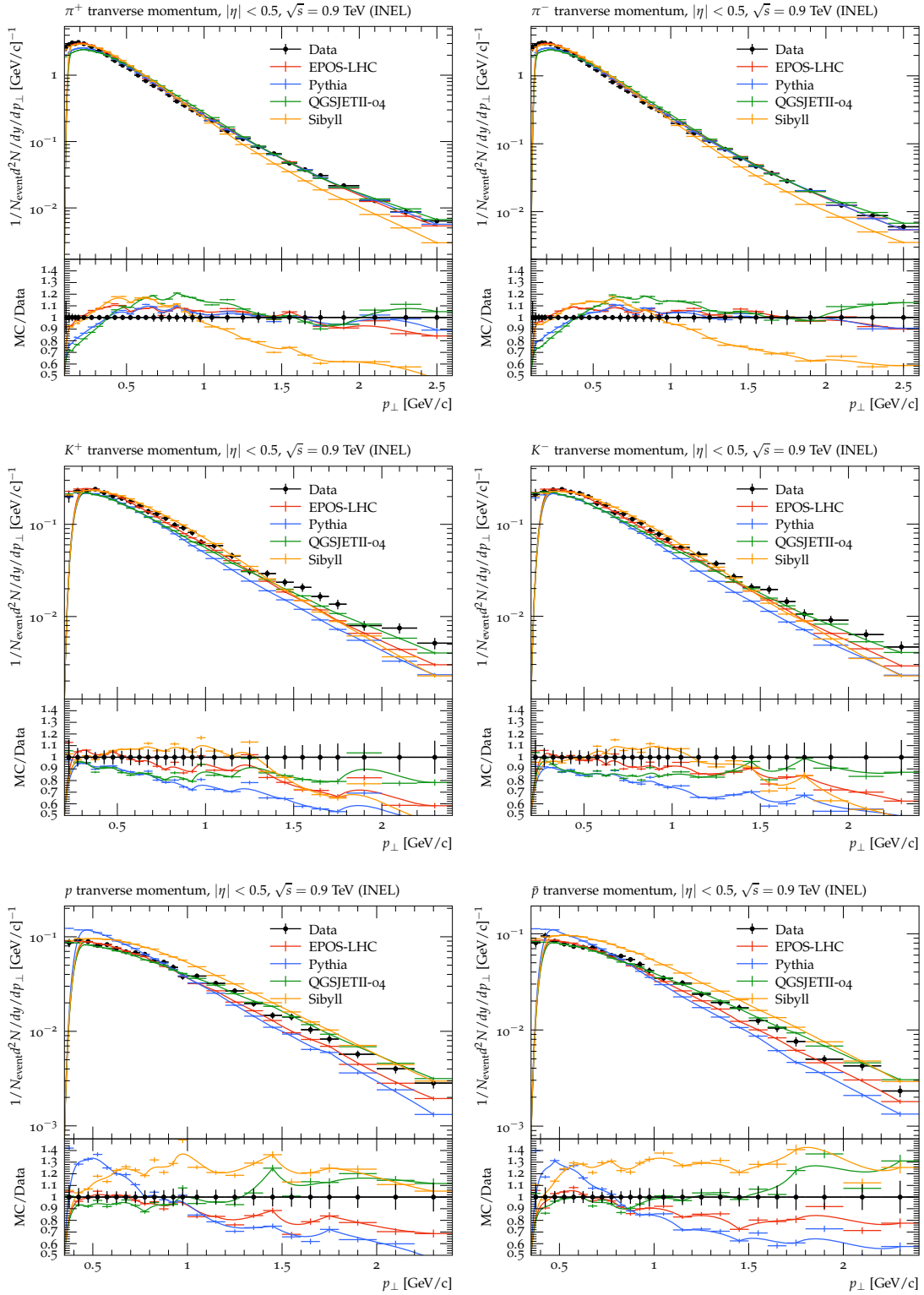


Figure 2: Transverse momentum spectra of the positively charged (left column) and negatively charged (right column) pions (first row) kaons (second row) and protons (third row) produced in pp collision at 900 GeV by EPOS-LHC, Pythia, QGSJET and Sibyll models are compared with the measurement of ALICE experiment. Filled black circles are used to represent experimental data while lines of different colors are used to show the models results as shown in the legend. The lower panel of the graph shows the ratio of the model to data.

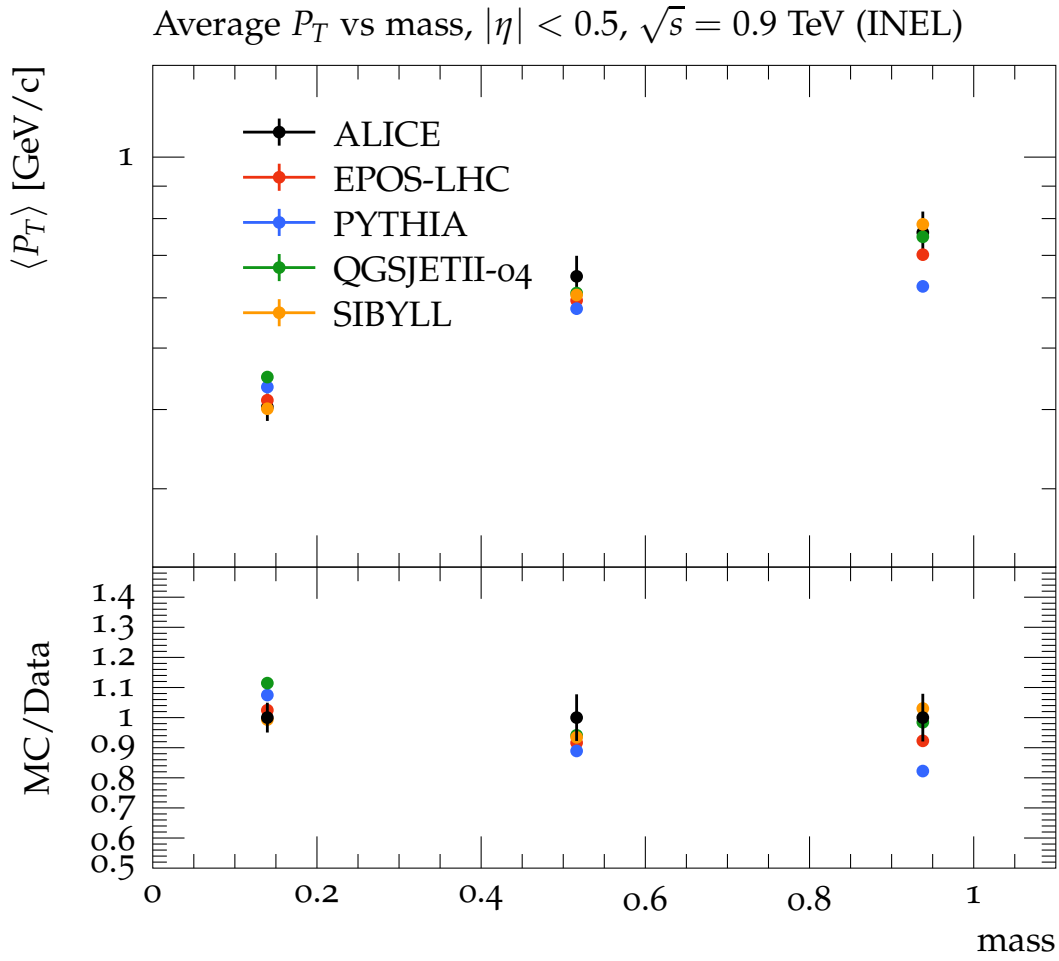


Figure 3: The average transverse momentum as a function of mass for the particles in the current study are shown for experimental data by filled black circles while filled circular markers of different colors are used for models predictions. The lower panel of the graph shows the ratio of the models to the experimental data.

of the graph. In case of experimental data, the vertical error bars are the quadrature addition of statistical and systematic errors, while in case of models predictions, the error bars represents statistical errors. Furthermore, the horizontal bar at a point is the width of the x-axis bin. The lower panel of the graph shows the ratio of the model to data. As can be seen from Figure 1, all the models with in the error bars can reproduce the π^\pm spectra very well over the entire p_T range except Sibyll which underestimates the data above 1 GeV/c by up to 40 %. In the low p_T range of less than 0.2 GeV/c, Pythia and QGSJET underestimate the data by up to 25 %. For K^\pm , the EPOS-LHC and QGSJET models reproduce the data up to 1.3 GeV/c with QGSJET describing the data for K^- meson over the entire p_T range. The other two models underestimate the data having increasing discrepancy with increasing p_T . The QGSJET model reproduce the protons and anti-protons spectra up to 1.4 GeV/c and 1.7 GeV/c respectively while the EPOS-LHC model could describe the data only at low p_T up to 0.9 GeV/c. Pythia and EPOS-LHC underestimate the data above 1 GeV/c while Sibyll overestimate the distribution over the entire p_T range.

Fig. 3 shows the variation of the average transverse momentum $\langle p_T \rangle$ as a function of the mass of the particles. The $\langle p_T \rangle$ is observed to be increasing with increasing mass of the particles. The behavior of increasing $\langle p_T \rangle$ with increasing the mass of the particle is well reproduced by all the models. Only the Pythia model underestimate the $\langle p_T \rangle$ for protons only.

2.2 Summary and Conclusions

Analyses of the transverse momentum spectra of identified charged particles are presented using modified Hagedorn function with embedded transverse flow velocity. The function fit the data approximately well indicated by the Data/Fit curves. We found that the average transverse flow velocity (β) decreases while the kinetic freezeout temperature

increases with increasing the mass of the particle. The same results has been reproduced by the models as well. For $p_T < 0.5$ GeV/ c , the function could not fit the data and model simulations very well. This is the region where most of the pions are produced by the decay of resonances – an effect that has not been considered in the function. for region with $p_T > 0.5$ GeV/ c , the function fit all the data very well. Simultaneously, the measurements performed by the ALICE experiment were compared by prediction of several event generator presented in the transverse momentum range of $p_T = 0.1$ – 2.5 GeV/ c and pseudorapidity $|\eta| < 0.5$ in pp collisions at $\sqrt{s} = 900$ GeV. Except Sibyll which underestimates the data above 1 GeV/ c by up to 40 %, all models with in the error bars reproduced the pions spectra well over the entire p_T range. The EPOS–LHC and QGSJET models reproduced the kaons spectra up to 1.3 GeV/ c with QGSJET describing the data for K^- meson over the entire p_T range. The other two models underestimate the data with a larger discrepancy with increasing p_T . The QGSJET model reproduce the p (\bar{p}) spectra up to 1.4 GeV/ c and 1.7 GeV/ c respectively while the EPOS–LHC model could describe the data only at low p_T up to 0.9 GeV/ c . The average transverse momenta of the particles increases with increasing the mass of the particle. The behavior of increasing average transverse momentum with increasing the mass of the particle is well reproduced by all the models. Only the Pythia model underestimated the average transverse momentum for protons only. Although all the model reproduced the measurements by the ALICE experiment for some of the particles or for a region of the momentum range, none of them reproduced the spectra for all the particles over the entire p_T range.

References

1. K. Akiba et. al., J. Phys. G **43** (2016) 110201,
2. CMS Collaboration, Eur. Phys. J. C **75** (2015) 237, doi:10.1140/epjc/s10052-015-3435-4,
3. ALICE Collaboration, Phys. Lett. B **736** (2014) 196, doi:10.1016/j.physletb.2014.07.011,
4. E. Schnedermann and J. Solfrank, Phys. Rev. C **48**, (1993) 2462
5. STAR Collab. (B. I. Abelev et al.), Phys. Rev. C **81**, (2010) 024911
6. H. L. Lao et al., Eur. Phys. J. A **53**, (2017) 44
7. T. Bhattacharyya et al., Eur. Phys. J. A **52**, (2016) 30
8. P. K. Khandai et al., J. Phys. G **41**, (2014) 025105
9. Kh. K. Olimov et al., Mod. Phys. Lett. A **35**, (2020) 2050237
10. Kh. K. Olimov et al., Mod. Phys. Lett. A **35**, (2020) 2050115
11. B. Abelev et al. (ALICE Collaboration), Phys. Rev. C **88**, (2013) 044910
12. M. Ajaz et. al., Int. J. Theor. Phys. **59** (2020), 3338
13. M. Ajaz, M. Tufail, and Y. Ali, Arab. J. Sci. Eng. **45**, (2020) 411 doi:10.1007/s13369-019-04224-8
14. Rashid Khan and Muhammad Ajaz, Mod. Phys. Lett. A. **35**, (2020) 2050190
15. M. Ajaz, R. Khan, Y. Ali, and M.K. Suleymanov, Mod. Phys. Lett. A. **35**, (2020) 1950349
16. S. Ullah, M. Ajaz, Z. Wazir, Y. Ali, K. H. Khan and H. Younis, Scientific Reports **9**, (2019) 11811
17. S. Ullah, M. Ajaz and Y. Ali EPL (Europhysics Letters) **123**, (2018) 31001
18. S. Ullah, Y. Ali, M. Ajaz, U. Tabassam and Q. Ali, Int. J. Mod. Phys. A **33**, (2018) 1850108
19. K. Aamodt et al. (ALICE Collaboration), Eur. Phys. J. C **71**, (2011) 1655
20. T. Pierog, I. Karpenko, J. M. Katzy, E. Yatsenko, K. Werner, Phys. Rev. C **92** (2015) 034906.
21. T. Sjostrand, S. Mrenna, and P. Skand, Pythia 6.4 Physics and manual, JHEP **05**, (2006) 026
22. S. Ostapchenko, Phys. Rev. D **83** (2011) 014018;
23. S. Ostapchenko, Nuclear Physics B - Proceedings Supplements, **151**, (2006) 143–146
24. Felix Riehn et. al., Phys. Rev. D **102**, 063002 (2020)
25. P K Khandai et al 2014 J. Phys. G: Nucl. Part. Phys. **41** 025105
26. K. Werner et. al., Phys. Rev. C **74**, 044902 (2006).
27. K. Werner Phys. Rev. Lett. **98**, 152301(2007).
28. A. B. Kaidalov and K. A. Ter-Martirosyan, Sov. J. Nucl. Phys. **39**, (1984) 979
29. M. Waqas et. al., Indian J. Phys. **93**, (2019) 1329-1343
30. M. Waqas et. al., Eur. Phys. J. A **56**, (2020) 188
31. M. Waqas et. al., Int. J. Mod. Phys E **30**, (2021) 2150061
32. M. Ajaz et. al., Results in Physics, **30**, (2021) 104790
33. M. Waqas et. al., J. Phy. G (Nucl. Part. Phys.) **48**, (2021) 075108